AD-A110 452 WISCONSIN UNIV-MADISON MATHEMATICS RESEARCH CENTER F/G 12/1
FORCED CONVECTION IN THREE-DIMENSIONAL FLOWS. III. ASYMPTOTIC S--ETC(U)
NOV 81 M A MCCLELLAND, W E STEWART DAAG29-80-C-0041
UNCLASSIFIED MRC-TSR-2295 NL

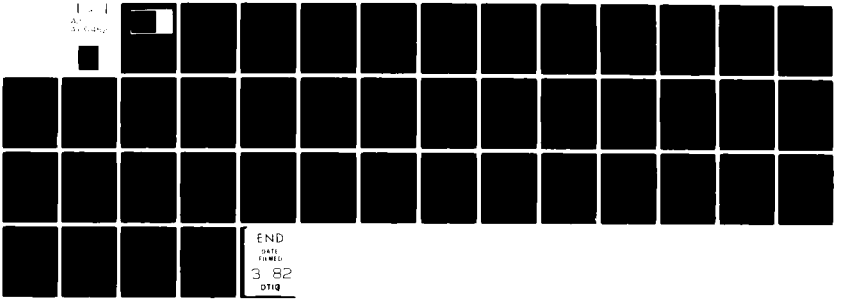

END
DATE FILMED
3-82
DTIC

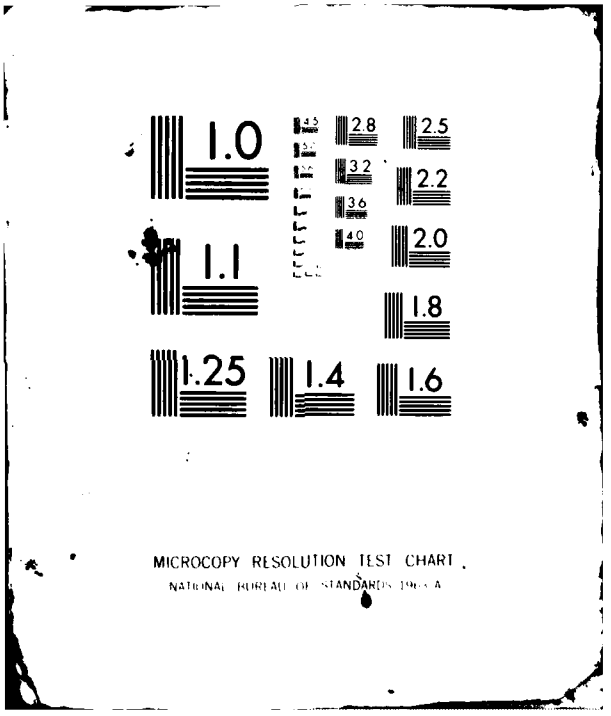
1.0
1.1
1.25
1.4
1.6
1.8
2.0
2.2
2.5
2.8
3.2
3.6
4.0
MICROCOPY RESOLUTION TEST CHART
NATIONAL BUREAU OF STANDARDS 1963-A

LEVEL II

(2)

AD A110452

MRC Technical Summary Report #2295

FORCED CONVECTION IN THREE-DIMENSIONAL FLOWS: III. ASYMPTOTIC SOLUTIONS WITH VISCOUS HEATING

Matthew A. McClelland and
Warren E. Stewart

Mathematics Research Center
University of Wisconsin—Madison
610 Walnut Street
Madison, Wisconsin 53706

November 1981

Received August 25, 1980

Approved for public release
Distribution unlimited

Sponsored by

U. S. Army Research Office
P. O. Box 12211
Research Triangle Park
North Carolina 27709

UNIVERSITY OF WISCONSIN - MADISON
MATHEMATICS RESEARCH CENTER

FORCED CONVECTION IN THREE-DIMENSIONAL FLOWS: III. ASYMPTOTIC SOLUTIONS WITH VISCOUS HEATING

Matthew A. McClelland and Warren E. Stewart

Technical Summary Report #2295
November 1981

ABSTRACT

Asymptotic solutions are given for temperature profiles in laminar three-dimensional flows with viscous dissipation. The results are asymptotically valid for small thermal diffusivity, and they hold for Newtonian or non-Newtonian fluids. The fluid properties are evaluated at an average temperature for the system; this is satisfactory for moderate temperature differences. Heat transfer formulas for various thermal boundary conditions are included. The general formulas are applied to several geometries; numerical results are obtained for a wire-coating operation.

AMS(MOS) Subject Classification: 35C20, 35K05, 76R05, 80A20

Key Words: Matched asymptotic solutions, Boundary layers, Viscous dissipation, Heat transfer

Work Unit No. 2 - Physical Mathematics

Sponsored by the United States Army under Contract No. DAAG29-80-C-0041.

SIGNIFICANCE AND EXPLANATION

In this paper we study the effect of viscous heating on the temperature distribution in a flowing liquid. Matched asymptotic solutions are obtained for the temperature distribution in the presence of viscous dissipation, with and without interfacial heat transfer. The results are asymptotically valid for small thermal diffusivity (large Prandtl number); they should prove useful in studies of wire coating, extrusion, heat transfer, and other flow processes with high rates of shear or highly viscous liquids.

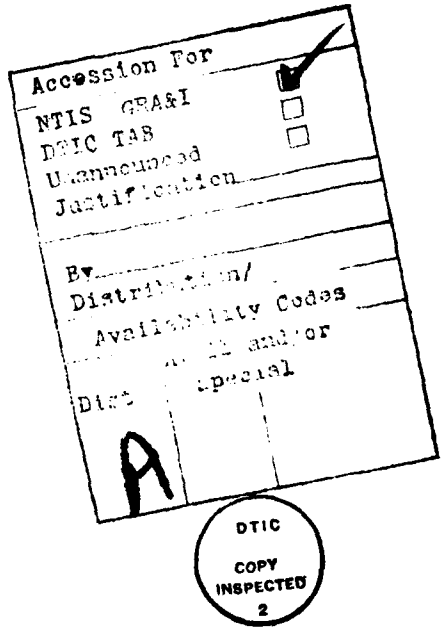

The responsibility for the wording and views expressed in this descriptive summary lies with MRC, and not with the authors of this report.

FORCED CONVECTION IN THREE-DIMENSIONAL FLOWS: III. ASYMPTOTIC SOLUTIONS WITH VISCOUS HEATING

Matthew A. McClelland and Warren E. Stewart

SCOPE

Small-diffusivity asymptotes have given useful information on a variety of heat and mass transfer systems. Part I and II of this series (Stewart, 1963; Stewart, Angelo and Lightfoot, 1970) dealt with boundary-layer phenomena in the absence of viscous heating. The present paper adds the effects of viscous heating in the boundary layers and in the main flow region. The results should prove useful in studies of wire-coating, extrusion, heat transfer, and other flow processes involving rapid deformation or highly viscous fluids.

This treatment holds for laminar non-separated regions of external flows, and for laminar thermal entrance regions of internal flows. The velocity profiles are considered as given or separately calculable; this is consistent with the use of an average temperature in evaluating the fluid properties.

Sponsored by the United States Army under Contract No. DAAG29-80-C-0041.

CONCLUSIONS

The key results of this analysis are the inner and outer solutions, given in Equations (46), (15), and (54). These may be combined with the superposition formulas of Papers I and II (Stewart, 1963; Stewart, Angelo and Lightfoot, 1970) to predict the temperature profiles and heat transfer rates in various three-dimensional flows once the velocity profiles are given. The resulting general formulas for steady-state systems are given in Eqs. (47) - (51).

For fluids with small thermal diffusivities, α, the enthalpy increase caused by viscous heating is of order $\alpha^{-1/3}$ in boundary layers that are steady as viewed from the nearest interfacial element. The increase is of order α^{0} in time-dependent boundary layers, and is of order α^{0} outside the boundary layers both for steady and unsteady flows. The order $\alpha^{-1/3}$ agrees with that found by Meksyn (1960) for the steady laminar boundary layer on a flat plate at high Prandtl numbers. A somewhat stronger dependence, $\alpha^{-1/2}$, holds for steady laminar boundary layers at Prandtl numbers near unity (Pohlhausen, 1921).

INTRODUCTION

For complex flows with viscous dissipation, it is difficult and time-consuming to solve the equations of change in full detail. However, useful asymptotes are obtainable for heat transfer by considering the limiting case of small thermal diffusivity.

Paper I (Stewart, 1963) gave asymptotic solutions for forced convection near fixed interfaces, with viscous dissipation neglected. The boundary layers considered there were at steady state when viewed from any interfacial element.

Paper II (Stewart et al., 1970) dealt with forced convection near mobile interfaces. The boundary layers considered there were time-dependent as viewed from the nearest interfacial element. The analysis included internal heat sources, but viscous dissipation was not explicitly treated.

In this work the results of Papers I and II are extended to include viscous dissipation. We use the continuity and energy equations for a constant-property fluid

$$(\nabla \cdot \underset{\sim}{v}) = 0 \tag{1}$$

$$\frac{DT}{Dt} - \alpha \nabla^2 T = - \frac{(\underset{\sim}{\tau} : \nabla \underset{\sim}{v})}{\rho C_p} \tag{2}$$

and treat the velocity field as given.

Particular integrals of Equation (2) are derived here as matched asymptotic solutions for the boundary layers and the main flow region. The complementary solutions from Papers I and II can be superimposed on these results, to describe the combined effects of interfacial heat transfer and viscous dissipation. We do the superposition explicitly for steady-state systems in Eqs. (47)-(51).

COORDINATES AND VELOCITIES

The steady-state inner (boundary layer) solution is done in the curvilinear coordinates x, y, and z of Paper I. The coordinate x is measured along the surface streamlines; simplifications for two-dimensional systems will be considered later. The coordinate y is the normal distance from the surface, and the surface coordinate z is measured normal to the local x-direction. In the neighborhood of a given interface these coordinates are orthogonal, with scale factors defined by

$$d\underset{\sim}{r} = \underset{\sim}{\delta}_x h_x \, dx + \underset{\sim}{\delta}_y h_y \, dy + \underset{\sim}{\delta}_z h_z \, dz \, . \tag{3}$$

The scale factor h_y is unity here, and h_x and h_z are taken at their interfacial values.

The steady-state outer (main flow) solution is done in streamline coordinates, illustrated in Figure 1. Each streamline is given by the intersection of two stream sheets of constant ψ_1 and ψ_2, and each point on a streamline is identified by ℓ, the arc length downstream from a reference surface.

The velocity components for the steady-state inner solution are taken from Paper I. They reduce to

$$v_x^{(i)} = y \, \beta(x,z) + O(y^2) \tag{4}$$

$$v_y^{(i)} = - \frac{y^2}{2h_x h_z} \frac{\partial}{\partial x} (h_z \beta) + O(y^3) \tag{5}$$

$$v_z^{(i)} = 0 + O(y^2) \tag{6}$$

in the absence of net mass transfer. These expressions satisfy Equation (1) to first order in y. The non-negative function β is the interfacial magnitude of the rate-of-strain tensor as defined by Bird, Armstrong and Hassager (1977); for brevity we call this quantity the interfacial shear

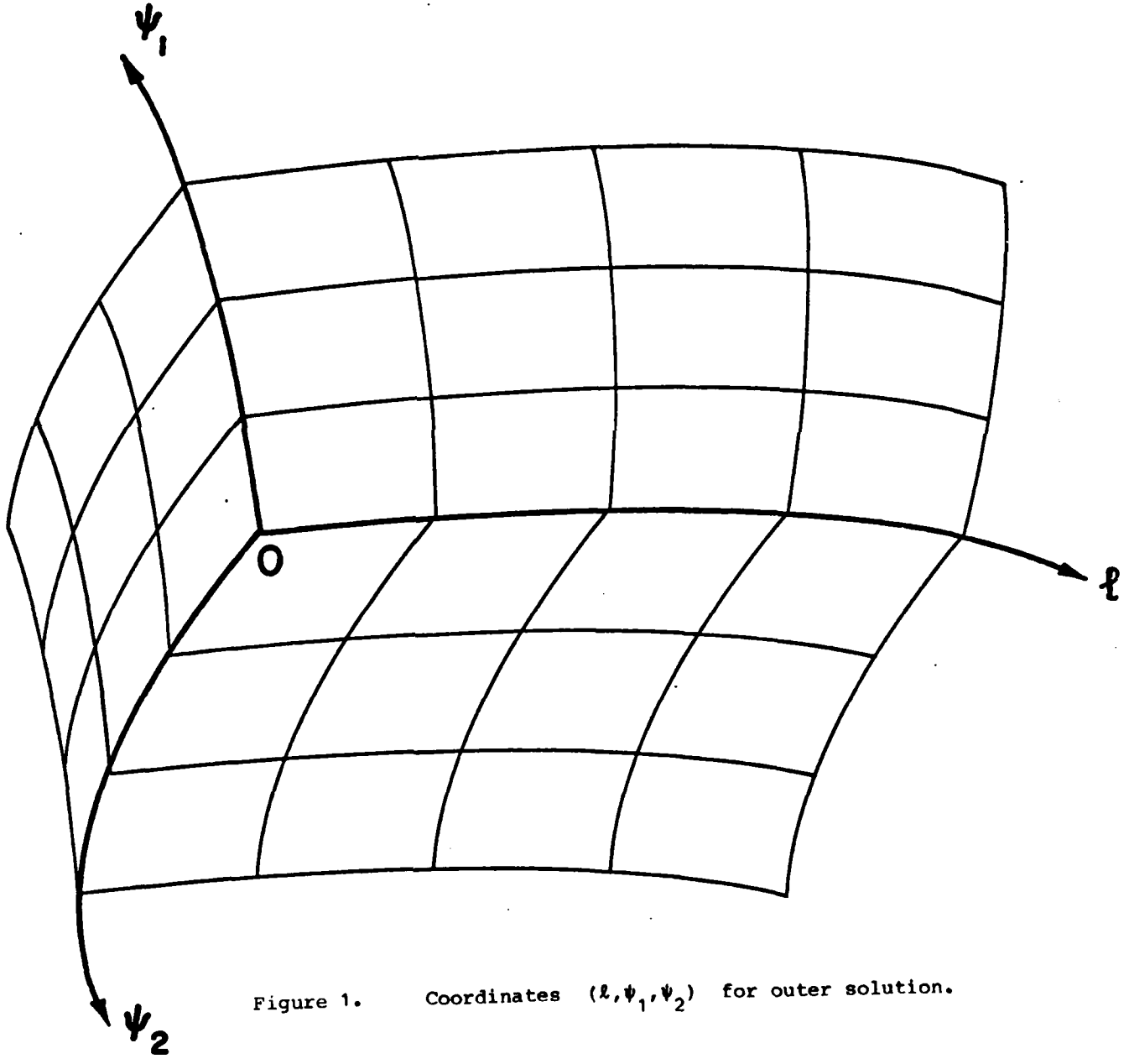

Figure 1. Coordinates (ℓ, ψ_1, ψ_2) for outer solution.

rate. A particular flow field is described (to the indicated order in y) by specifying the surface coordinate grid and the function $\beta(x,z)$.

For the subsequent matching of inner and outer solutions, we need to express Equation (4) in the coordinates of Figure 1. The continuity equation is automatically satisfied by setting

$$\underset{\sim}{v} = [\nabla \psi_1 \underset{\sim}{\times} \nabla \psi_2] \tag{7}$$

which may be applied in the boundary layer coordinates (x,y,z) to give

$$\underset{\sim}{v}^{(i)} = \begin{vmatrix} \underset{\sim}{\delta}_x & \underset{\sim}{\delta}_y & \underset{\sim}{\delta}_z \\ \frac{1}{h_x}\frac{\partial \psi_1}{\partial x} & \frac{1}{h_y}\frac{\partial \psi_1}{\partial y} & \frac{1}{h_z}\frac{\partial \psi_1}{\partial z} \\ \frac{1}{h_x}\frac{\partial \psi_2}{\partial x} & \frac{1}{h_y}\frac{\partial \psi_2}{\partial y} & \frac{1}{h_z}\frac{\partial \psi_2}{\partial z} \end{vmatrix} \tag{8}$$

This expression agrees with Equations (4), (5), and (6) if we take the stream functions in the forms

$$\psi_1 = \frac{y^2}{2} h_z \beta + O(y^3) \tag{9}$$

$$\psi_2 = z + C + O(y) \tag{10}$$

with C an arbitrary constant. Hence, Equation (4) can be rewritten

$$v_x^{(i)} = \sqrt{2 \psi_1 \beta / h_z} + O(\psi_1) . \tag{11}$$

OUTER SOLUTION FOR STEADY FLOWS

At a distance from the boundaries, the heat conduction term of Equation (2) can be neglected as $\alpha \to 0$. For steady-state conditions this equation then becomes

$$\hat{\rho C_p}(\underset{\sim}{v} \cdot \nabla T^{(o)}) = -(\underset{\sim}{\tau} : \nabla \underset{\sim}{v}) \tag{12}$$

which may be rewritten in the streamline coordinates as

$$\hat{\rho C_p}\, v \frac{\partial T^{(o)}}{\partial \ell} = -(\underset{\sim}{\tau} : \nabla \underset{\sim}{v}) \ . \tag{13}$$

Integration of this equation with the initial condition

$$T = T_\infty \quad \text{at} \quad \ell = 0 \tag{14}$$

yields the outer temperature profile

$$T^{(o)}(\ell, \psi_1, \psi_2) - T_\infty = \frac{1}{\hat{\rho C_p}} \int_0^{\ell} \frac{-(\underset{\sim}{\tau} : \nabla \underset{\sim}{v})}{V} d\ell_1 \tag{15}$$

which is well-behaved, except near stationary boundaries where V vanishes and $(\underset{\sim}{\tau}:\nabla \underset{\sim}{v})$ does not. Near such boundaries, heat conduction becomes important and an inner solution is required.

The subsequent matching of solutions will require the asymptote of Equation (15) as $\psi_1 \to 0$. To order $\sqrt{\psi_1}$ we may set $V = v_x^{(i)}$, $d\ell = h_x dx$, and

$$-(\underset{\sim}{\tau} : \nabla \underset{\sim}{v}) \doteq \tau_0(x,z)\beta \tag{16}$$

in which $\tau_0(x,z)$ is the wall shear stress. The resulting asymptote of Equation (14) near stationary boundaries is

$$\lim_{\psi_1 \to 0} \sqrt{2\psi_1}\, [T^{(o)}(\ell, \psi_1, \psi_2) - T_\infty] = \frac{1}{\hat{\rho C_p}} \int_0^{x} \tau_0 \sqrt{h_z \beta}\, h_x dx_1 \tag{17}$$

with $\ell = \int_0^x h_x dx_1$ in this limit.

INNER SOLUTION FOR STEADY FLOWS

Equation (2) can be simplified according to the usual boundary layer approximations (Schlichting, 1960; Rosenhead, 1963). In the limit of small α, the Laplacian $\nabla^2 T$ reduces essentially to the second normal derivative, $\frac{\partial^2 T}{\partial y^2}$. In the same limit, Equation (16) describes the viscous dissipation in the boundary layer. With these substitutions, and use of Equations (4), (5) and (6), the energy equation becomes

$$\frac{y\beta}{h_x}\frac{\partial T^{(i)}}{\partial x} - \frac{y^2}{2h_x h_z}\frac{\partial}{\partial x}(h_z\beta)\frac{\partial T^{(i)}}{\partial y} = \alpha\frac{\partial^2 T^{(i)}}{\partial y^2} + \frac{\tau_0\beta}{\rho C_p} \qquad (18)$$

for steady-state boundary layers in the limit of small α. Since no z-derivatives remain, Equation (18) can be integrated in two dimensions with z as a parameter.

Eq. (18) can be solved conveniently by representing $\tau_0\beta$ as a superposition of special functions $\varepsilon(x,\xi,z)$. Each ε-function has a different value of the location parameter ξ, and vanishes for $x < \xi$. A corresponding family of solutions $T^{*(i)}$ is defined by the differential equation

$$\frac{y\beta}{h_x}\frac{\partial T^{*(i)}}{\partial x} - \frac{y^2}{2h_x h_z}\frac{\partial}{\partial x}(h_z\beta)\frac{\partial T^{*(i)}}{\partial y} = \alpha\frac{\partial^2 T^{*(i)}}{\partial y^2} + \frac{\varepsilon(x,\xi,z)}{\rho C_p}, \qquad (19)$$

and the boundary conditions

$$\frac{\partial T^{*(i)}}{\partial y} = 0 \qquad \text{at} \quad y = 0 \qquad (20)$$

$$T^{*(i)} \to T_\infty \qquad \text{as} \quad y \to \infty \qquad (21)$$

$$T^{*(i)} = T_\infty \qquad \text{for} \quad x < \xi\,. \qquad (22)$$

Once the functions $\varepsilon(x,\xi,z)$ are found, these and the resulting solutions $T^{*(i)}$ can be superimposed to solve Equation (18) for an adiabatic boundary.

We postulate the following form for $T^{*(i)}$,

$$T^{*(i)} - T_\infty = f(x,\xi,z)q(\eta) \tag{23}$$

with

$$\eta = \frac{y}{\delta(x,\xi,z)} . \tag{24}$$

Here $\delta(x,\xi,z)$ is a boundary layer thickness, which [in view of Eq. (22)] is taken to vanish for $x < \xi$. The boundary conditions (20) and (21) then reduce to

$$\frac{dq}{d\eta} = 0 \quad \text{at} \quad \eta = 0 \tag{25}$$

$$q \to 0 \quad \text{as} \quad \eta \to \infty . \tag{26}$$

Insertion of the postulates (23) and (24) into Equation (19) gives

$$\left[\frac{\delta^3\beta}{\alpha h_x f} \frac{\partial f}{\partial x} \right]\eta q - \left[\frac{\delta^2\beta}{\alpha h_x} \frac{\partial \delta}{\partial x} + \frac{\delta^3}{2\alpha h_x h_z} \frac{\partial}{\partial x}(h_z\beta) \right]\eta^2 \frac{dq}{d\eta} = \frac{d^2q}{d\eta^2} + \left[\frac{\delta^2\varepsilon}{kf} \right] . \tag{27}$$

The postulates hold only if the bracketted terms are independent of x, for $x \geq \xi$:

$$\frac{\delta^2\beta}{\alpha h_x} \frac{\partial \delta}{\partial x} + \frac{\delta^3}{2\alpha h_x h_z} \frac{\partial}{\partial x}(h_z\beta)$$

$$\equiv \frac{\delta^2\sqrt{h_z\beta}}{\alpha h_x h_z} \frac{\partial}{\partial x}(\delta\sqrt{h_z\beta}) = C_0(z) \tag{28}$$

$$\frac{\delta^3\beta}{\alpha h_x} \frac{\partial \ln f}{\partial x} = C_1(z) \tag{29}$$

$$\frac{\delta^2\varepsilon}{kf} = C_2(z). \tag{30}$$

The functions $C_i(z)$ may be chosen as positive constants. Choosing $C_0 = 3$ and integrating Equation (28) with the initial condition

$$\sqrt{h_z \beta}\ \delta(x,\xi,z) = 0 \qquad \text{at} \quad x = \xi \tag{31}$$

required by Eq. (22), we obtain the boundary layer thickness

$$\delta = \frac{1}{\sqrt{h_z \beta}} \left\{ 9\alpha \int_{\xi}^{x} \sqrt{h_z \beta}\ h_x h_z\, dx_1 \right\}^{1/3} \qquad (x \geq \xi). \tag{32}$$

The choice $C_2 = 1$ gives

$$f = \delta^2 \varepsilon / k \ . \tag{33}$$

Equations (28) and (29) give the following differential equation for f :

$$\frac{\partial \ell n\, f}{\partial x} = \frac{C_1}{C_0} \frac{\partial \ell n (\delta \sqrt{h_z \beta})}{\partial x} \qquad (x \geq \xi) \tag{34}$$

Let $C_1/C_0 = r = \text{constant}$; then Equation (34) may be integrated to give

$$f = C_3 (\delta \sqrt{h_z \beta})^r \qquad (x \geq \xi). \tag{35}$$

The value of C_1 is determined by matching the inner and outer solutions for the region $x > \xi$. The outer limit of the inner solution has the form

$$\lim_{\eta \to \infty} \{\eta [T^{*(i)} - T_\infty]\} = \frac{f}{(C_0 + C_1)} \tag{36}$$

according to Equations (23) and (27)-(30). Insertion of Equation (35) gives

$$\lim_{\eta \to \infty} \{\eta [T^{*(i)} - T_\infty]\} = \frac{C_3\, \delta^r (h_z \beta)^{r/2}}{(C_0 + C_1)} \ . \tag{37}$$

The inner limit, Equation (17), of the outer solution may be rewritten for the source distribution $\varepsilon(x,\xi,z)$ to give

$$\lim_{\psi_1 \to 0} \{\sqrt{2\psi_1}\ [T^{*(o)} - T_\infty]\} = \frac{1}{\rho C_p} \int_{\xi}^{x} \varepsilon \sqrt{h_z/\beta}\ h_x dx_1 \ . \tag{38}$$

Here ξ has replaced zero as the lower limit of integration. Insertion of Equations (9), (33) and (35) gives

$$\lim_{y \to 0} \{y [T^{*(o)} - T_\infty]\} = \frac{C_3 \alpha}{\sqrt{h_z \beta}} \int_{\xi}^{x} h_x h_z \delta^{r-2} (h_z \beta)^{\frac{r-1}{2}} dx_1 \ . \tag{39}$$

For $r = 2$ and $C_1 = 6$, Equations (37) and (39) match, giving

$$\lim_{y\to\infty} \{y[T^{*(i)} - T_\infty]\} = \lim_{y\to 0} \{y[T^{*(o)} - T_\infty]\} = \frac{C_3 \delta^3 h_z \beta}{9} . \qquad (40)$$

Equation (27) then becomes

$$6\eta g - 3\eta^2 \frac{dg}{d\eta} = \frac{d^2 g}{d\eta^2} + 1 \qquad (41)$$

which may be solved numerically with boundary conditions (25) and (26). The resulting surface value of the function g is

$$g(0) = 0.32973 \qquad (42)$$

and the function $g(\eta)$ is shown in Figure 2.

The constant C_3 of Equation (35) remains to be determined. Equations (33) and (35) give, for $r = 2$,

$$C_3 = \frac{\varepsilon}{k h_z \beta} \qquad (x \geq \xi) . \qquad (43)$$

By definition, ε vanishes for $x < \xi$; thus, $\varepsilon/h_z\beta$ is a step function. Insertion of Equations (43), (32), and (35) with $r = 2$ into Equation (23) then gives

$$T^{*(i)} - T_\infty = \frac{9^{2/3}}{\rho C_p \alpha^{1/3}} g(\eta) \left(\int_{x_1=\xi}^{x} \sqrt{h_z \beta}\, h_x h_z dx_1 \right)^{2/3} \frac{\varepsilon}{h_z \beta} \qquad (44)$$

as the fundamental inner solution.

We now return to the solution of Equation (18) with an adiabatic boundary at $y = 0$, a uniform upstream temperature T_∞ for $x < 0$, and an arbitrary shear stress distribution $\tau_0(x,z)$ for $x \geq 0$. The amplitudes of the step functions $\varepsilon/h_z\beta$ are now chosen by specifying

$$\frac{\tau_0}{h_z} = \int_{\xi=0_-}^{x} d\left(\frac{\tau_0}{h_z}\right) \Bigg|_{\xi,z} = \int_{\xi=0_-}^{x} d\left(\frac{\varepsilon}{h_z \beta}\right) \Bigg|_{\xi,z} \qquad (45)$$

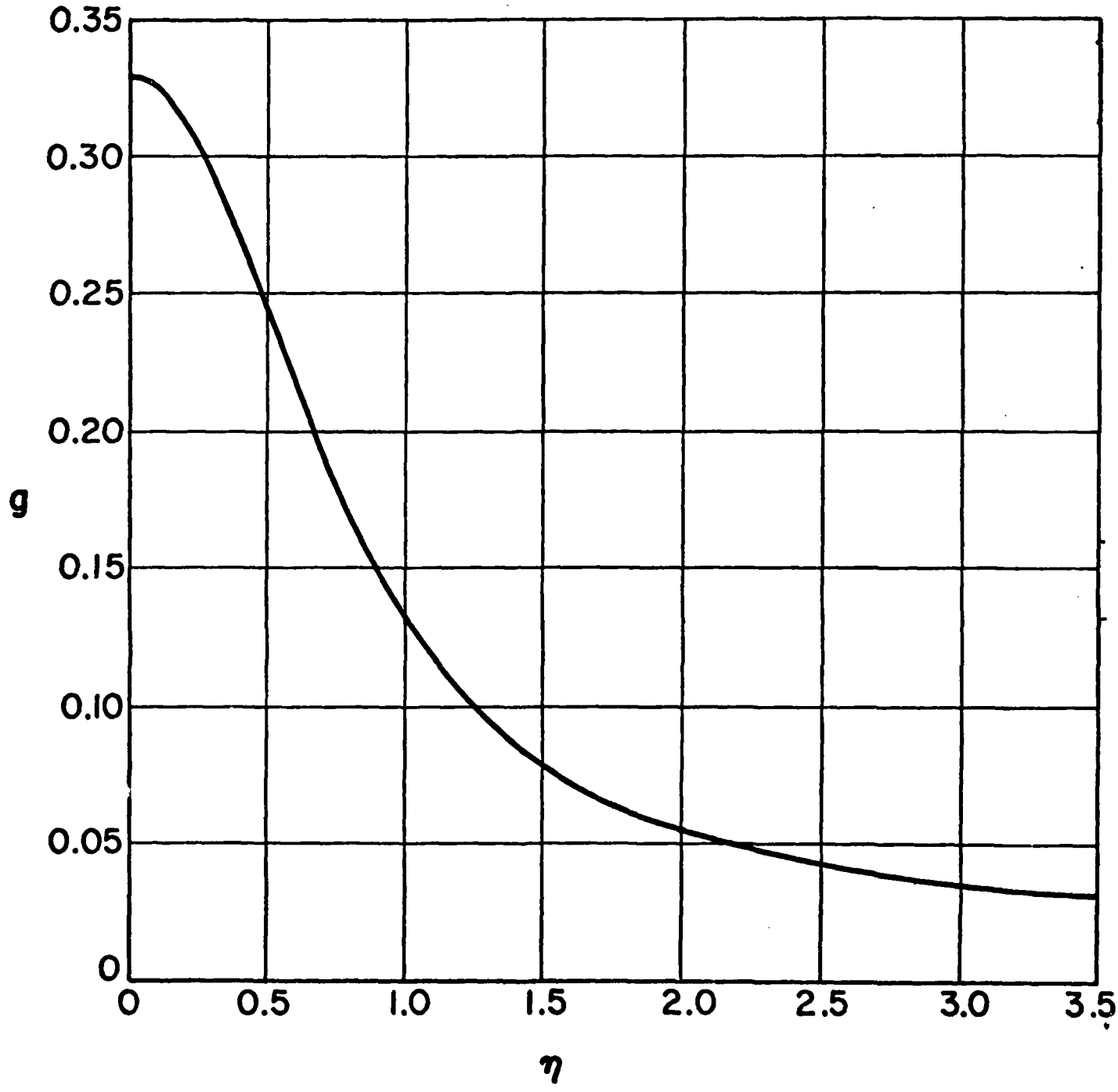

Figure 2. Boundary layer temperature function $g(\eta)$; solution of Equations (25), (26), and (41).

thus equating the steps to increments of τ_0/h_z . Doing likewise in Equation (44) and superimposing the results, we obtain the inner solution

$$T_A^{(i)} - T_\infty = \frac{9^{2/3}}{\rho C_p \alpha^{1/3}} \int_{\xi=0_-}^{x} g(\eta)\Big(\int_{x_1=\xi}^{x} \sqrt{h_z \beta}\, h_x h_z dx_1 \Big)^{2/3} d\Big(\frac{\tau_0}{h_z}\Big) \Bigg|_{\xi,z} . \quad (46)$$

for the case of an adiabatic boundary. The outer limit of this solution matches the inner limit of Equation (15). The outer integrations in Eqs. (45) and (46) are begun from $\xi = 0_-$, with τ_0 initally zero to conform to the ε-functions.

Results for non-adiabatic boundaries may be obtained by combining the present results with those of Stewart (1963). In that work Equation (2) was solved without the dissipation term, with a uniform upstream temperature T_∞ and with arbitrary interfacial thermal conditions for $x \geq 0$. Since Eq. (2) is linear, we may superimpose Eq. (25) of the 1963 paper upon the particular solution just found; this gives the following temperature profile for the case of a given surface temperature distribution $T_0(x,z)$:

$$T(x,y,z) = T_A(x,y,z) + \int_{0_-}^{x} [1 - \Pi(\eta)]\big|_{\xi,x,y,z}\, d(T_0 - T_{0,A})\big|_{\xi,z} . \quad (47)$$

Here $T_{0,A}$ is obtained from Eq. (46) with $y = 0$; also

$$\Pi(\eta) = \frac{1}{\Gamma(4/3)} \int_0^{\eta} \exp(-\eta_1^3)\, d\eta_1 \quad (48)$$

with η defined by Equations (24) and (32). The resulting interfacial heat flux is

$$q_0 = -k\frac{\partial T}{\partial y}\Big|_{y=0}$$

$$= \frac{k\sqrt{h_z \beta}}{(9\alpha)^{1/3}\Gamma(4/3)} \int_{\xi=0_-}^{x} \Big\{ \int_{x_1=\xi}^{x} \sqrt{h_z \beta}\, h_x h_z dx_1 \Big\}^{-1/3} d(T_0 - T_{0,A})\big|_{\xi,z} \quad (49)$$

and the total heat transfer rate through a surface region $0 \leq x < x_2(z)$, $z_I < z < z_{II}$ is

$$Q = \frac{3^{1/3}k}{2\Gamma(4/3)\alpha^{1/3}} \int_{z_I}^{z_{II}} \int_{\xi=0_-}^{x_2(z)} \left\{ \int_{x_1=\xi}^{x_2(z)} \sqrt{h_z \beta}\, h_x h_z dx_1 \right\}^{2/3} d(T_0 - T_{0,A})\Big|_{\xi,z}. \quad (50)$$

A two-dimensional version of Eq. (49) was given by Lighthill (1950), but with an approximate function $T_{0,A}$ based on the calculations of Pohlhausen (1921) for Prandtl numbers near unity. The present results are preferable for large Prandtl numbers.

The temperature profile corresponding to any given surface heat flux distribution $q_0(x,z)$ is obtained by combining Eq. (46) above with Eq. (39) of Stewart (1963):

$$T(x,y,z) = T_A(x,y,z) + \frac{1}{\frac{1}{3}\Gamma(\frac{2}{3})\,\rho C_p (9\alpha)^{2/3}} \int_{0_-}^{x} \frac{\exp(-\eta^3) q_0 h_x h_z\, d\xi}{\left[\int_{\xi}^{x} \sqrt{h_z \beta}\, h_x h_z dx_1\right]^{2/3}}. \quad (51)$$

This completes the steady-state solutions to lowest order in α.

TRANSIENT SOLUTIONS

For transient processes, an outer solution for $\alpha \to 0$ is obtained by starting from Equation (2) without the conduction term:

$$\rho \hat{C}_p \frac{DT^{(o)}}{Dt} = - (\underset{\sim}{\tau} : \nabla \underset{\sim}{v}) \ . \tag{52}$$

The initial condition is taken to be

$$T(X_1, X_2, X_3, t) = T_\infty \quad \text{at} \quad t = 0 \ . \tag{53}$$

Here the X_i are material coordinates. Integration along the particle paths gives the time-dependent outer solution

$$T^{(o)}(X_1, X_2, X_3, t) - T_\infty = \frac{1}{\rho C_p} \int_0^t -(\underset{\sim}{\tau} : \nabla \underset{\sim}{v})\Big|_{X_1, X_2, X_3, t_1} dt_1 \tag{54}$$

which reduces to Equation (15) for steady flows.

The transient inner solution for the dissipative temperature rise is obtainable from Equation (80) of Paper II. In the limit of small α, the dissipation term of Eq. (2) may be approximated in the boundary layer by the local interfacial value. The resulting inner solution for T is independent of the normal coordinate y, and is consequently unaffected by heat conduction. Equation (54) matches this adiabatic inner solution exactly at the interface, and is preferable everywhere else. Thus, for adiabatic time-dependent systems with small α, Equation (54) is valid throughout the fluid. This particular integral [with $T^{(o)}$ labelled as T_A] can be superimposed with Eqs. (76)-(79) of Paper II to describe unsteady-state heat transfer with viscous dissipation. An application of Eq. (54) is given in the final example.

APPLICATIONS TO SIMPLE GEOMETRIES

The flows considered in this section are Newtonian and have uniform temperature upstream from a locus $x = 0$ where significant dissipation begins. Inner solutions are presented for adiabatic boundaries; these may be superimposed with Equations (49) and (51) to obtain results for other interfacial boundary conditions.

Developed Flows in Ducts

For slow flows of viscous liquids in ducts, the hydrodynamic development region may be considerably shorter than the thermal entrance region. The temperature profiles may then be approximated by assuming abrupt flow development at the entrance of the duct. The x-coordinate for these systems is measured parallel to the flow axis and the z-coordinate is measured around the duct perimeter. The scale factors h_x and h_z are set equal to unity. Several duct geometries are shown in Figure 3, and the corresponding expressions for β are shown in Table 1. Equation (46) gives the inner solution for the temperature rise,

$$T_A^{(i)} - T_\infty = \frac{(81\nu^2 \, Pr \, x^2 \, \beta^4)^{1/3}}{C_p^*} \, g\left(y \sqrt[3]{\frac{\beta}{9\alpha x}} \right) \qquad (55)$$

and the outer solution is obtainable from Equation (15).

Wedge Flows

Consider a laminar two-dimensional flow impinging on the wedge shown in Figure 4. The boundary-layer coordinates are rectangular with $h_x = 1$. The velocity profiles are given by Hartree (1937); the interfacial shear rate is

$$\beta = f''(0,m)\left(\frac{m+1}{2} \frac{U^3}{\nu x} \right)^{1/2} \qquad (x > 0) \qquad (56)$$

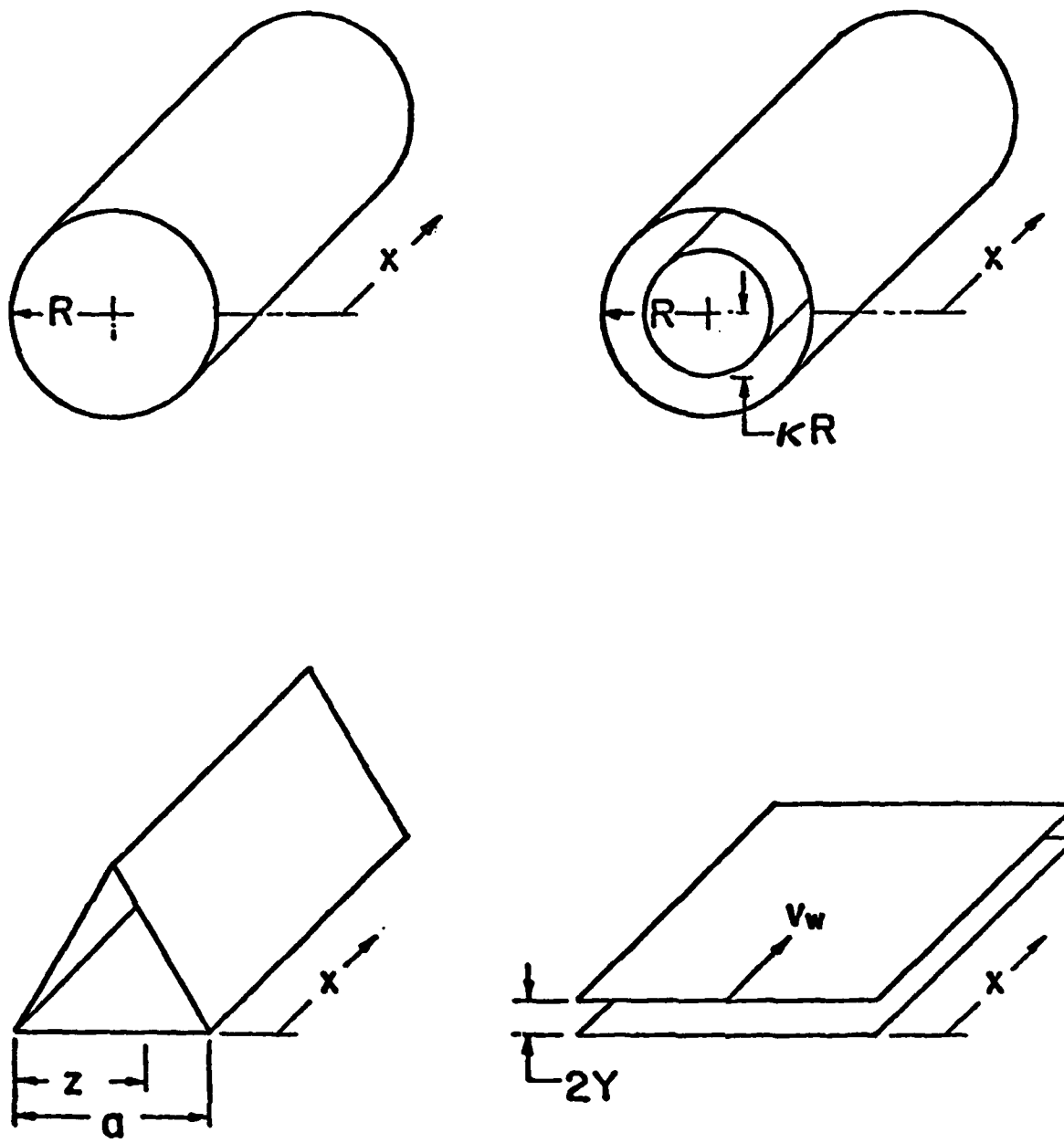

Figure 3. Duct geometries: tube, annulus, equilateral three-walled duct, and slit with one wall moving downstream.

TABLE 1

WALL SHEAR RATES FOR FULLY DEVELOPED NEWTONIAN FLOWS IN DUCTS

Duct Geometry	Wall shear rate, β
Tube	$(P_0 - P_L)R/2\mu L$
Annulus: Inner Cylinder	$\frac{(P_0 - P_L)R}{2\mu L}\left[-\kappa - \frac{(1+\kappa^2)}{2\ln(1/\kappa)}\frac{1}{\kappa}\right]$
Outer Cylinder	$\frac{(P_0 - P_L)R}{2\mu L}\left[1 - \frac{(1-\kappa^2)}{2\ln(1/\kappa)}\right]$
Equilateral Three-walled Duct (Landau and Lifshitz, 1960)	$\frac{\sqrt{3}\,(P_0 - P_L)}{2\mu L}\frac{z(a-z)}{a}$
Slit with One Wall Moving Downstream:	
Fixed Wall	$\frac{(P_0 - P_L)Y}{\mu L} + \frac{V_w}{2Y}$
Moving Wall	$\left\lvert\frac{(P_0 - P_L)Y}{\mu L} - \frac{V_w}{2Y}\right\rvert$

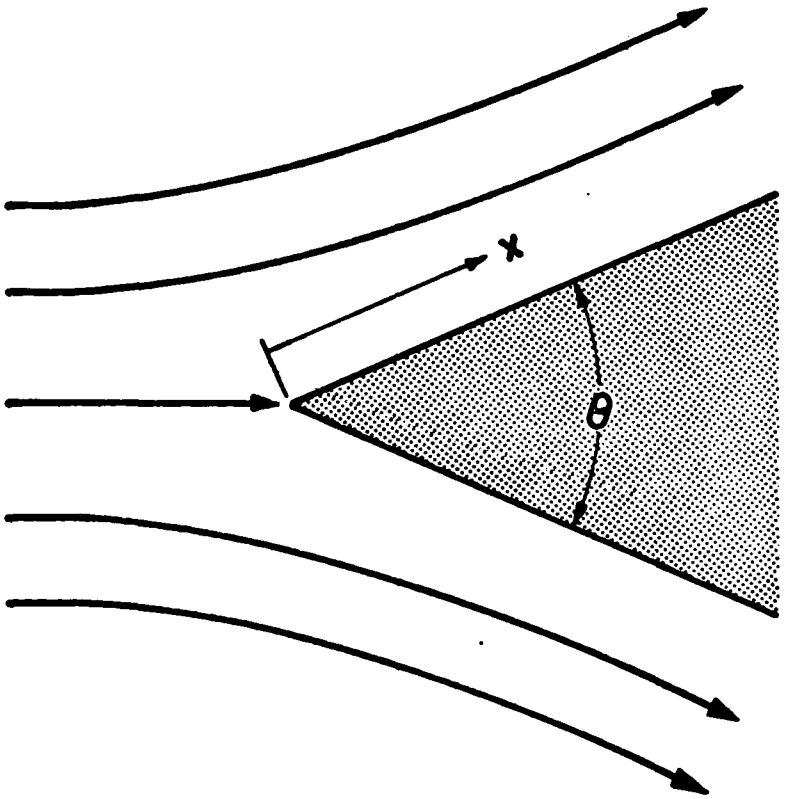

Figure 4. Laminar flow over a wedge.

Here U is the longitudinal velocity at the outer edge of the boundary layer,

$$U = u_1 x^m \tag{57}$$

and the exponent m is given by potential flow theory as

$$m = \theta/(2\pi-\theta) \ . \tag{58}$$

The dimensionless wall stress $f''(0,m)$ is tabulated by Hartree; some values are $f''(0,0) = 0.4696$ for the flat plate and $f''(0,1) = 1.233$ for plane stagnation flow. Equation (46) gives the following surface temperature distribution for flow over an adiabatic wedge, when note is taken of the jump in β (and thus in τ_0/h_z) at $x = 0$:

$$T_{0,A}^{(i)} - T_\infty = \left\{\frac{2}{3}\, 6^{2/3}\left[f''(0,m)\right]^{4/3} g(0) B\left(\frac{2}{3}, \frac{9m+1}{3m+3}\right)\right\} \frac{U^2 Pr^{1/3}}{\hat{C}_p} \ . \tag{59}$$

For the special case of a flat plate ($m = 0$), the resulting recovery factor is

$$\frac{\hat{C}_p\left[T_{0,A}^{(i)} - T_\infty\right]}{\frac{1}{2} U^2} = 1.92\ Pr^{\frac{1}{3}} \tag{60}$$

in agreement with the asymptote obtained by Meksyn (1960) for $Pr \gg 1$ for this geometry.

Creeping Flow Around a Sphere

Consider the steady creeping flow of a Newtonian fluid past a stationary sphere. The surface streamlines are contours of constant longitude ϕ, running from $\theta = 0$ to $\theta = \pi$ in spherical coordinates. The surface coordinates for the inner solution are $x = \theta$ and $z = \phi$, with scale factors $h_x = R$ and $h_z = R \sin\theta$. The Stokes velocity profile gives the interfacial shear rate

$$\beta = \frac{3}{2}\frac{V_\infty \sin\theta}{R}. \tag{61}$$

Thus, τ_0/h_z is a step function, vanishing for $x < 0$ and equal to $3\mu V_\infty/2R^2$ for $x > 0$. Equation (46) gives the dissipative temperature rise

$$T_{0,A}^{(i)} - T_\infty = \left(\frac{9}{4}\right)^{\frac{4}{3}} g(0) \frac{Pr^{\frac{1}{3}}}{C_p} \left[\frac{\nu}{R} V_\infty^2 (2\theta - \sin 2\theta)\right]^{\frac{2}{3}} \tag{62}$$

on the surface of an adiabatic sphere.

Slow Flow Around a Cylinder

Consider the slow steady flow of an infinite fluid across a circular cylinder of radius R. The surface streamlines run from $\theta = 0$ to $\theta = \pi$. The surface coordinates for the inner solution are $x = \theta$ and $z = Z$, with scale factors $h_x = R$ and $h_z = 1$, where (r,θ,Z) are the cylindrical coordinates. A series expression for the velocity profile near the cylinder is given by Rosenhead (1963). Using only the leading terms, one obtains the interfacial shear rate

$$\beta = \frac{2V_\infty \sin\theta}{SR}. \tag{63}$$

Here

$$S = \frac{1}{2} - \gamma + \ln(8\, Re^{-1}) \tag{64}$$

and γ is Euler's constant. Equation (46) gives the surface temperature rise due to viscous dissipation

$$T_{0,A}^{(i)} - T_\infty = \left(\frac{1296\, Pr\, \nu^2 V_\infty^4}{R^2 S^4}\right)^{\frac{1}{3}} \frac{g(0)}{C_p} \int_{\xi=0}^{\theta} \left(\int_{\theta_1=\xi}^{\theta} \sin^{\frac{1}{2}}\theta_1 d\theta_1\right)^{\frac{2}{3}} \cos\xi d\xi \tag{65}$$

in the absence of heat exchange between the cylinder and fluid. The double integral $I(\theta)$ has been evaluated numerically and is given in Table 2.

TABLE 2

INTEGRAL IN EQ. (65) FOR CYLINDER SURFACE TEMPERATURE

$180\ \theta/\pi$	$I(\theta) = \int_{\xi=0}^{\theta} \left(\int_{\theta_1=\xi}^{\theta} \sin^{1/2}\theta_1 d\theta_1 \right)^{2/3} \cos\xi d\xi$
0*	0.0000
15	0.0355
30	0.1377
45	0.2951
60	0.4896
75	0.6993
90	0.9008
105	1.073
120	1.198
135	1.267
150	1.278
165	1.243
180	1.195

*Stagnation line.

Flow Near a Rotating Disk

Consider the three-dimensional axisymmetric flow induced by a disk rotating with an angular velocity ω in an otherwise quiescent fluid. A cylindrical coordinate system is chosen which rotates with the disk. From the analysis of Cochran (1934) the surface velocity components are

$$V_r = r\,\omega\,F(\zeta) \tag{66}$$

$$V_\theta = r\,\omega\,[G(\zeta) - 1] \tag{67}$$

with

$$\zeta = Z\sqrt{\frac{\omega}{\nu}}\ . \tag{68}$$

From Cochran's tables of the solution, we obtain

$$\beta = \left.\frac{\partial V_t}{\partial Z}\right|_{Z=0} = \left.\frac{\partial}{\partial Z}\left(V_r^2 + V_\theta^2\right)^{\frac{1}{2}}\right|_{Z=0}$$

$$= r\sqrt{\omega^3/\nu}\ \sqrt{[F'(0)]^2 + [G'(0)]^2} \tag{69}$$

with $F'(0) = 0.510$ and $G'(0) = -0.616$.

Since the temperature is independent of θ , we choose r and θ as surface coordinates (x,z) for the inner solution, whence $h_x = 1$ and $h_z = r$. This is simpler than integration along the spiral surface streamlines, and gives the same result. The fundamental solution is then done with V_θ omitted, and with β replaced by $\beta_r = r\sqrt{\omega^3/\nu}\,F'(0)$ [see Equation (69)] except in calculation of the viscous dissipation. In Equations (45) and (46), we must accordingly replace $\varepsilon/h_z\beta$ by $\varepsilon/h_z\beta_r$, and τ_0/h_z by $\tau_0\beta/h_z\beta_r$. The resulting inner solution for the dissipative temperature rise is

$$T_A^{(i)} - T_\infty = \frac{(\omega r)^2}{\hat{C}_p}\,\frac{(9\,Pr)^{1/3}}{[F'(0)]^{2/3}}\,\{[F'(0)]^2 + [G'(0)]^2\}\,g\left(Z\sqrt[3]{\frac{F'(0)\omega^{3/2}}{3\,\alpha\,\nu^{1/2}}}\right) \tag{70}$$

for a thermally insulated disk.

Entrance Flow in a Tube

Consider a fluid which enters a circular tube of radius R with an initially flat velocity profile. From the numerical results of Hornbeck (1964), the quantity

$$f\,Re = \frac{-4R}{\langle V\rangle}\left.\frac{\partial v_z}{\partial r}\right|_{r=R} \tag{71}$$

is available as a function of downstream distance.

A curve fit of the numerical solutions plotted in Figure 5 gives the expression

$$f\,Re = \frac{1.328\,\sigma^{-\frac{1}{2}} + 452\,\sigma^{1.1} + 15.6}{1 + 28.25\,\sigma^{1.1}} \tag{72}$$

in which

$$\sigma = (x/R)(R\langle V\rangle/\nu)^{-1} . \tag{73}$$

Equation (72) satisfies the asymptotic relations

$$\lim_{\sigma\to 0} f\,Re = 1.328\,\sigma^{-\frac{1}{2}} \tag{74}$$

$$\lim_{\sigma\to\infty} f\,Re = 16 . \tag{75}$$

Equation (46), (71) and (72) give the surface temperature rise in the thermal entrance region of an adiabatic tube:

$$T_{0,A}^{(i)} - T_\infty = \frac{(\frac{9}{16})^{\frac{2}{3}}\, g(0)\, Pr^{\frac{1}{3}} \langle V\rangle^2}{\hat{C}_p} \int_{\xi=0_-}^{\sigma} \left(\int_{\sigma_1=\xi}^{\sigma} \sqrt{f\,Re}\; d\,\sigma_1 \right)^{\frac{2}{3}} d(f\,Re)\Big|_\xi . \tag{76}$$

This solution is plotted in dimensionless form in Figure 6. Near the entrance, the temperature rise is essentially that of the flat plate, whereas downstream the curve approaches the asymptote for hydrodynamically developed laminar flow.

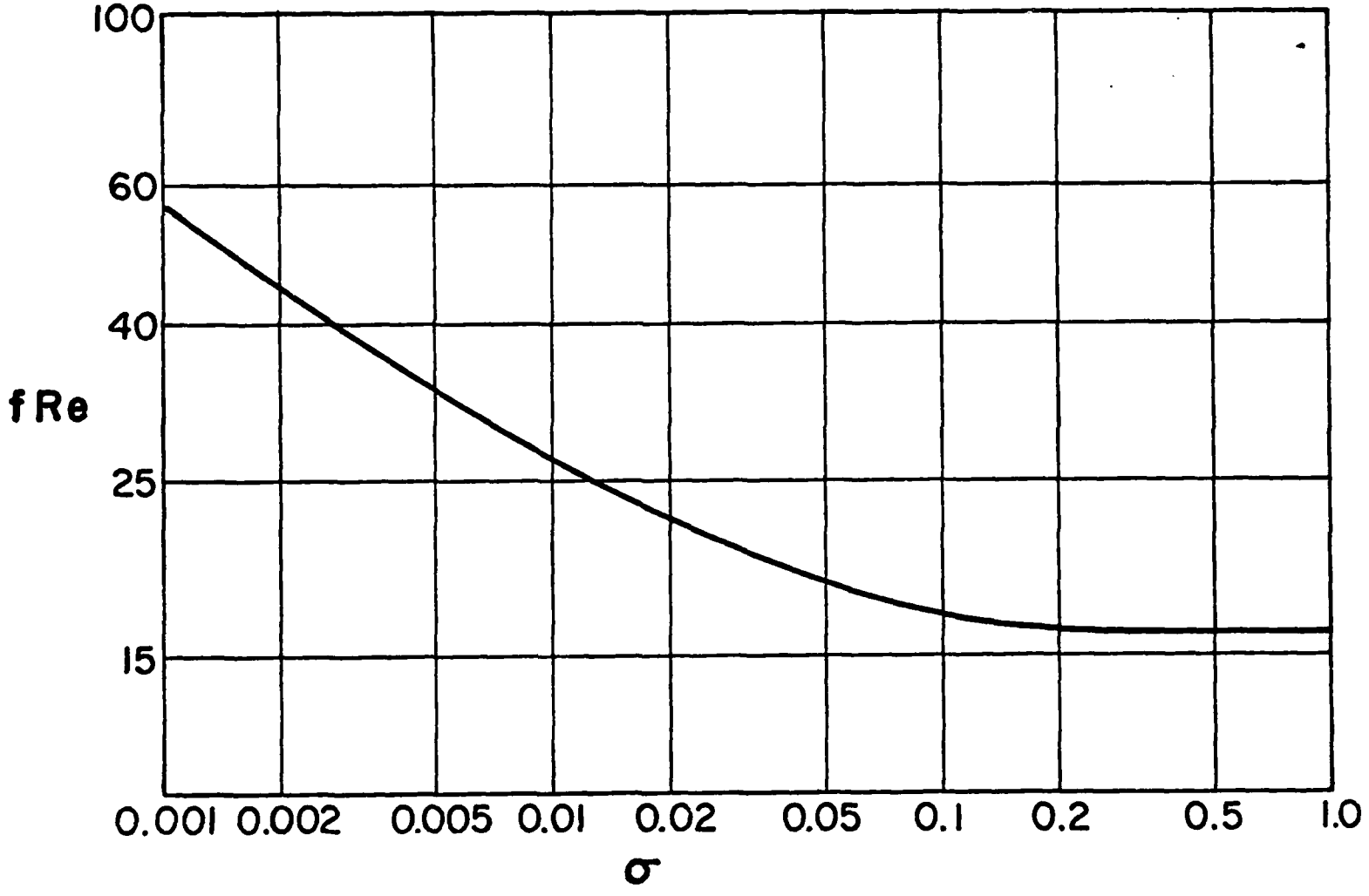

Figure 5. Wall shear stress function for entrance flow in a tube, according to Equation (71).

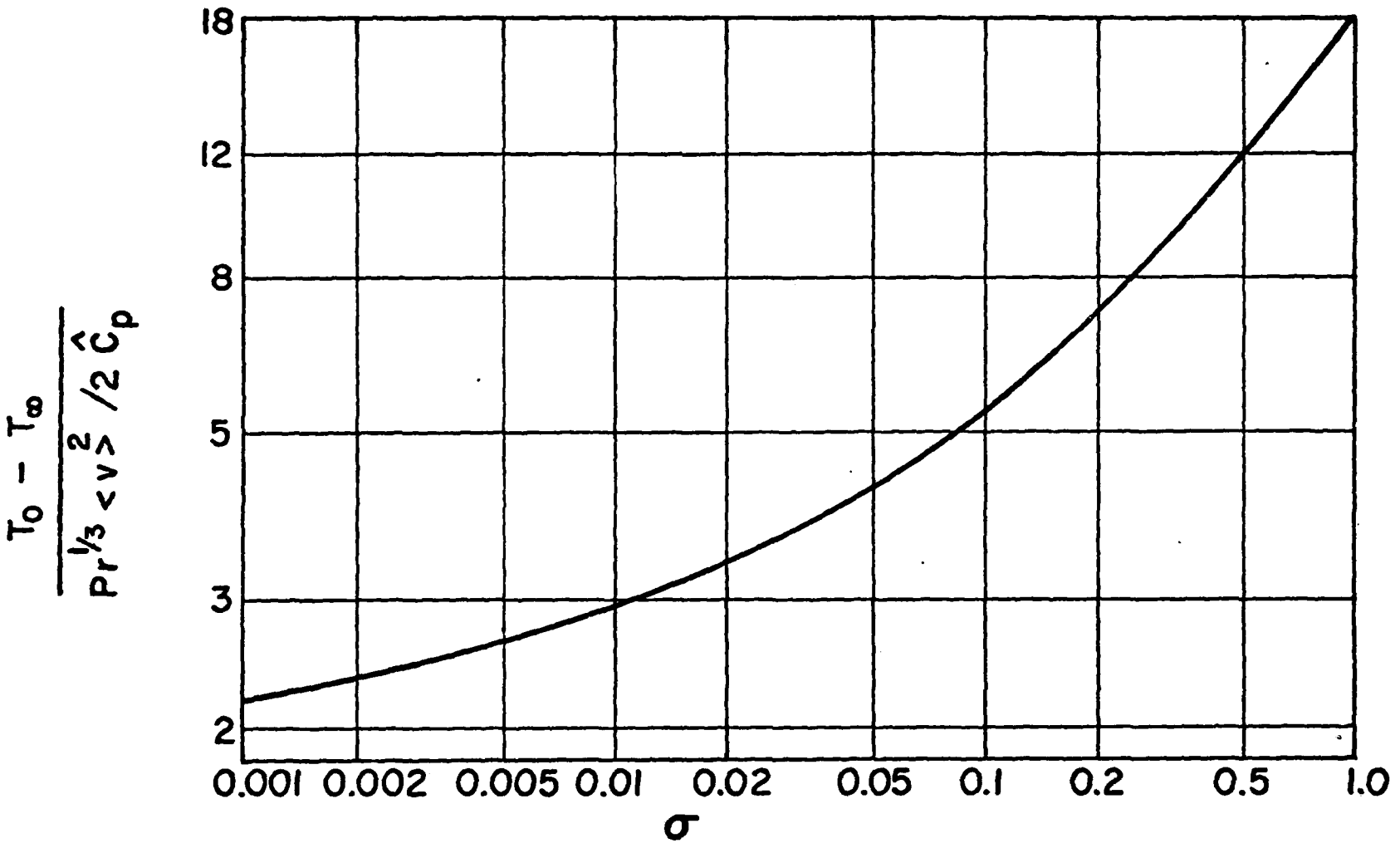

Figure 6. Wall temperature rise for adiabatic entrance flow in a tube.

A WIRE-COATING PROBLEM

Improvements in wire-coating processes have been made largely by empirical means. Experimental studies of such flows are difficult, because of the small clearances required in a wire-coating die. Theoretical treatment is hampered by temperature-dependent properties, along with complicated rheology and geometry. Previous theoretical work, summarized by Carley, Endò, and Krantz (1978), has included approximate analytical treatments and elaborate numerical computations. In this section we give an asymptotic analysis of a representative wire-coating process.

The geometry (see Figure 7) and operating conditions of a typical wire-coating die are given by Haas and Skewis (1974). The die wall is tapered, with local radius

$$R_2(x) = a(x)R_1. \qquad (77)$$

Here R_1 is the wire diameter, and

$$a(x) = a(0)\left(1 - \frac{x}{L}\right) + a(L)\left(\frac{x}{L}\right) \qquad (78)$$

with

$$a(0) = 3.39$$

$$a(L) = 1.17$$

$$L = 0.39 \text{ in. } (0.99 \text{ cm})$$

$$R_1 = 0.0127 \text{ in. } (0.0323 \text{ cm})$$

The coordinate x is the axial distance from the inlet of the die. The wire velocity V_w is 4000 ft. min^{-1} = 2032 cm S^{-1}.

An exact description of the flow field would require numerical integration of the coupled mass, momentum, and energy equations. Here an approximate velocity profile is used. The axial velocity profile in the melt is approximated by a three-term expansion

$$\frac{V_x}{V_w} = f_0(x) + f_1(x)\ln\left(\frac{r}{R_1}\right) + f_2(x)\left(\frac{r}{R_1}\right)^2 \qquad (79)$$

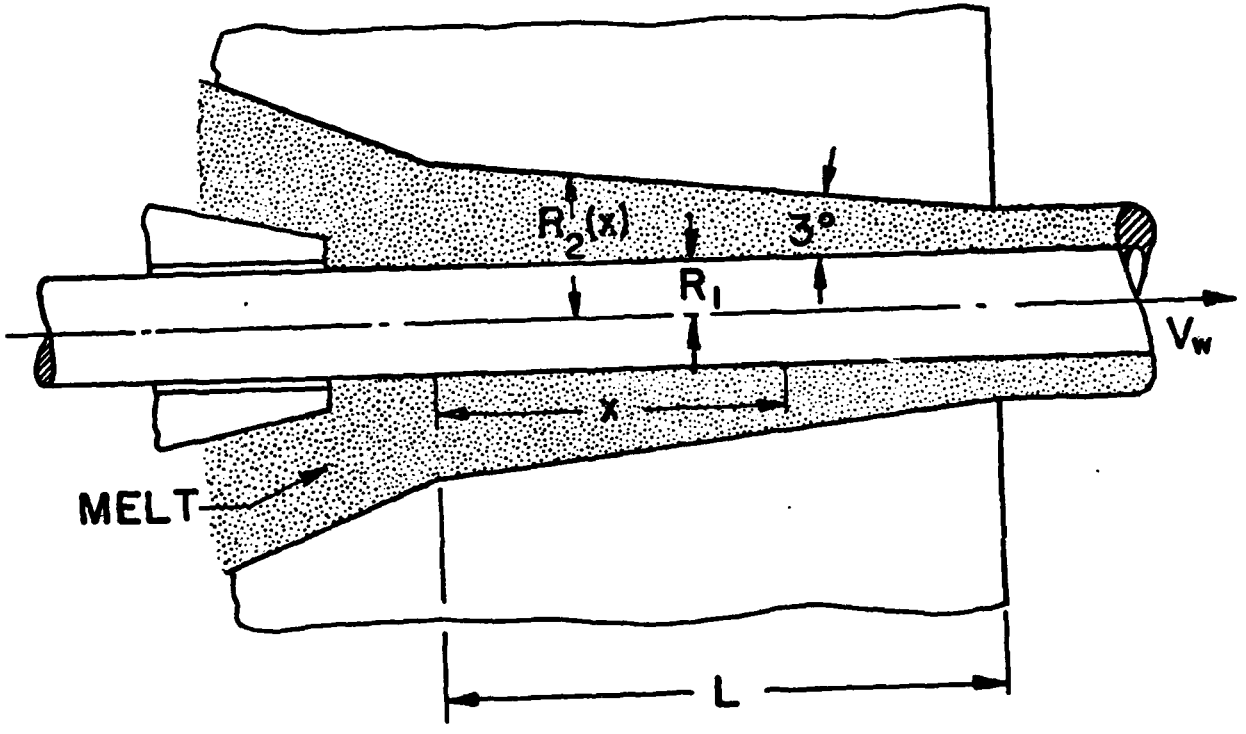

Figure 7. Schematic view of a wire-coating die.

based on functions appropriate to annular Newtonian flow with a moving inner cylinder. Use of the no-slip conditions at the interfaces,

$$V_x = V_w \quad \text{at} \quad r = R_1 \tag{80}$$

$$V_x = 0 \quad \text{at} \quad r = a(x)R_1 \tag{81}$$

and the given mass flow rate,

$$w = 2\pi\rho \int_{R_1}^{aR_1} V_x r dr \tag{82}$$

leads to three equations in the three unknowns:

$$f_0(x) + f_2(x) = 1 \tag{83}$$

$$f_0(x) + f_1(x) \ln a(x) + f_2(x)a^2(x) = 0 \tag{84}$$

$$a^2(L) - 1 = \int_1^{a(x)} 2(f_0(x) + f_1(x) \ln u + f_2(x)u^2)udu \, . \tag{85}$$

Here w has been chosen so that there is no draw-down, i.e., the final coating diameter matches the exit diameter of the die.

From Equation (79) the shear rates at the die wall and the wire surface are

$$\beta_d = \left| \frac{V_w}{R_1} \left[\frac{f_1(x)}{a(x)} + 2a(x)f_2(x) \right] \right| \tag{86}$$

$$\beta_w = \left| \frac{V_w}{R_1} \left[f_1(x) + 2f_2(x) \right] \right| \tag{87}$$

These functions are plotted in Figure 8. The shear rate at the die wall rises monotonically to a maximum of 3.3×10^5 sec^{-1}, while the shear rate at the wire first declines to zero and then rises to 2.1×10^5 sec^{-1}. In the entrance region, the fluid velocities do not exceed the wire velocity. In the exit region, however, fluid velocities greater than the wire velocity must occur to satisfy the zero draw-down specification.

Carley, Endo, and Krantz (1978) have provided property data for a representative low-density polyethylene melt. For the boundary regions, they use the shear stress model

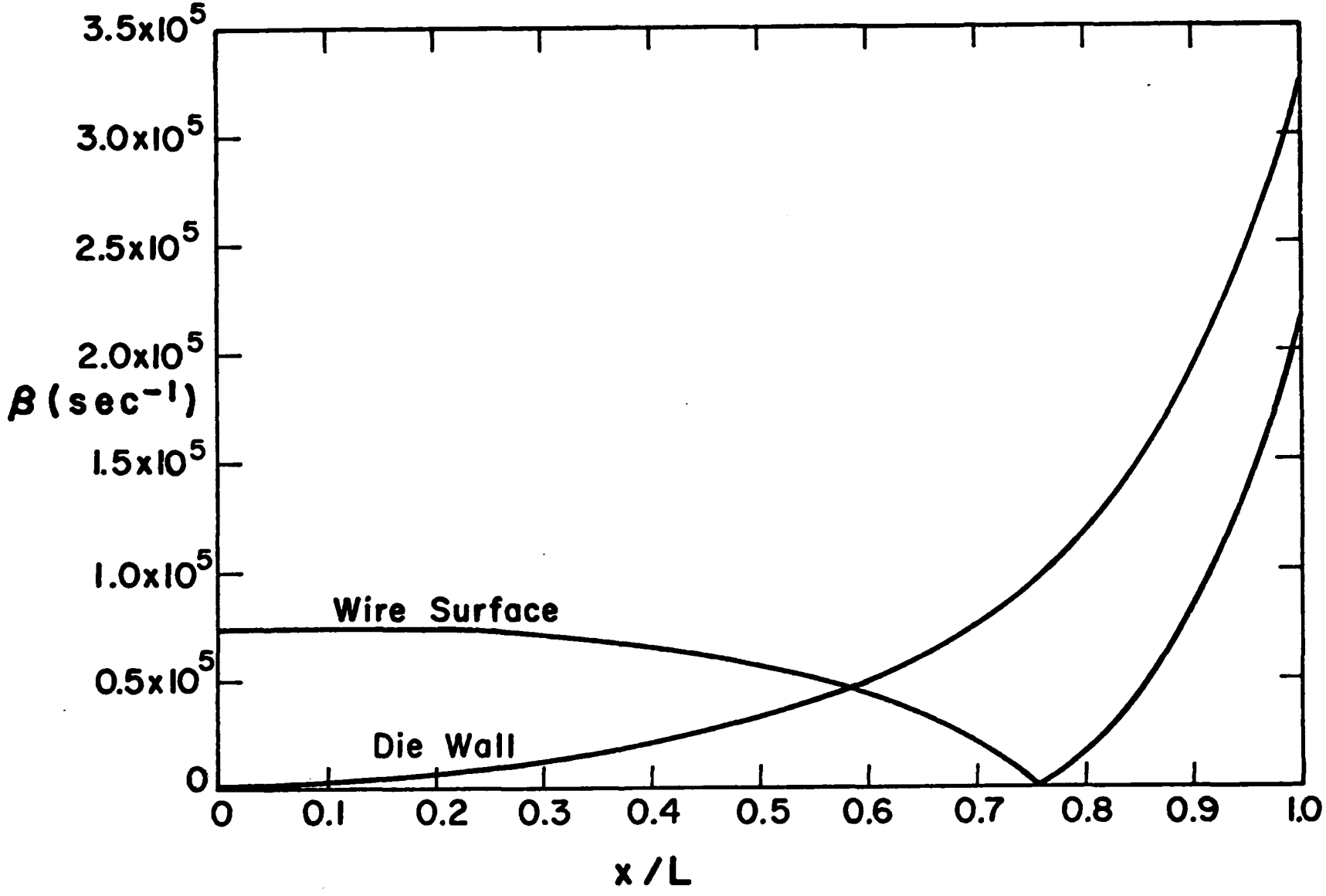

Figure 8. Approximate surface shear rates for a wire-coating operation.

$$\tau_{rz} = -m_T \left| \frac{dV_z}{dr} \right|^{-2/3} \frac{dV_z}{dr} \tag{88}$$

with

$$m_T = m_0 \exp \left[\frac{E}{R} \left(\frac{1}{T} - \frac{1}{T_{ref}} \right) \right] \tag{89}$$

and

$$m_0 = 101{,}000 \quad g\ cm^{-1}\ sec^{-5/3}$$

$$E = 11{,}700 \quad cal\ mole^{-1}$$

$$R = 1.987 \quad cal\ mole^{-1}\ K^{-1}$$

$$T_{ref} = 479\ K\ .$$

In this analysis m_T is taken as a constant, and is evaluated as described below. The following properties are treated as independent of temperature:

$$k = 0.000786 \quad cal\ sec^{-1}\ cm^{-1}\ K^{-1}$$

$$\rho = 0.91\ g\ cm^{-3}$$

$$\hat{C}_p = 0.55 \quad cal\ g^{-1}\ K^{-1}\ .$$

The surfaces of the wire-coating system are assumed adiabatic. At the die wall we use $h_x \doteq 1$ and $h_z = a(x)R_1$. Equations (46), (86), and (88) then give the die wall temperature distribution

$$T_0^{(i)} - T_\infty = \frac{9^{2/3}}{\hat{\rho C_p}} \frac{g(0)}{\alpha^{1/3}} \; m_T \left\{ \left(\int_{x_1=0}^{x} \sqrt{a\beta_d}\; a\, dx_1 \right)^{2/3} \left(\frac{\beta_d^{1/3}}{a} \right) \Bigg|_{\xi=0} \right.$$

$$\left. + \int_{\xi=0}^{x} \left(\int_{x_1=\xi}^{x} \sqrt{a\beta_d}\; a\, dx_1 \right)^{2/3} d\left(\frac{\beta_d^{1/3}(\xi)}{a(\xi)} \right) \right\} . \qquad (90)$$

for adiabatic operation. The first term of Equation (90) accounts for the assumed initial jump in wall shear rate, and the second term accounts for all subsequent changes. The index m_T is evaluated from Equation (89) at the mean of the entrance and exit surface temperatures; this entails an iterative calculation.

The temperature rise at the moving wire surface is obtained from Equations (54), (87) and (88), with $t = x/V_w$ and $-(\underset{\sim}{\tau} : \nabla \underset{\sim}{v}) = \tau_0 \beta_w$. The result is

$$T_0^{(o)} - T_\infty = \frac{m_T}{\rho C_p V_w} \int_{x_1=0}^{x} \beta_w^{\frac{4}{3}}\, dx_1 . \qquad (91)$$

The index m_T is again evaluated at the mean of the entrance and exit surface temperatures. Equation (15) is equivalent to Eq. (54) here since the system is at steady state when viewed from the die.

Numerical integration of Equations (90) and (91) with $T_\infty = T_{ref}$ gives the results shown in Figure 9 . The temperature at the die wall rises from 479K to 534K; this increase is comparable to the results obtained numerically by Carley, Endo, and Krantz (1978) for similar wire-coating systems. The calculated temperature rise at the wire surface is much smaller (only 5.8K at the maximum) and becomes still less if one allows for heat transfer to the moving wire.

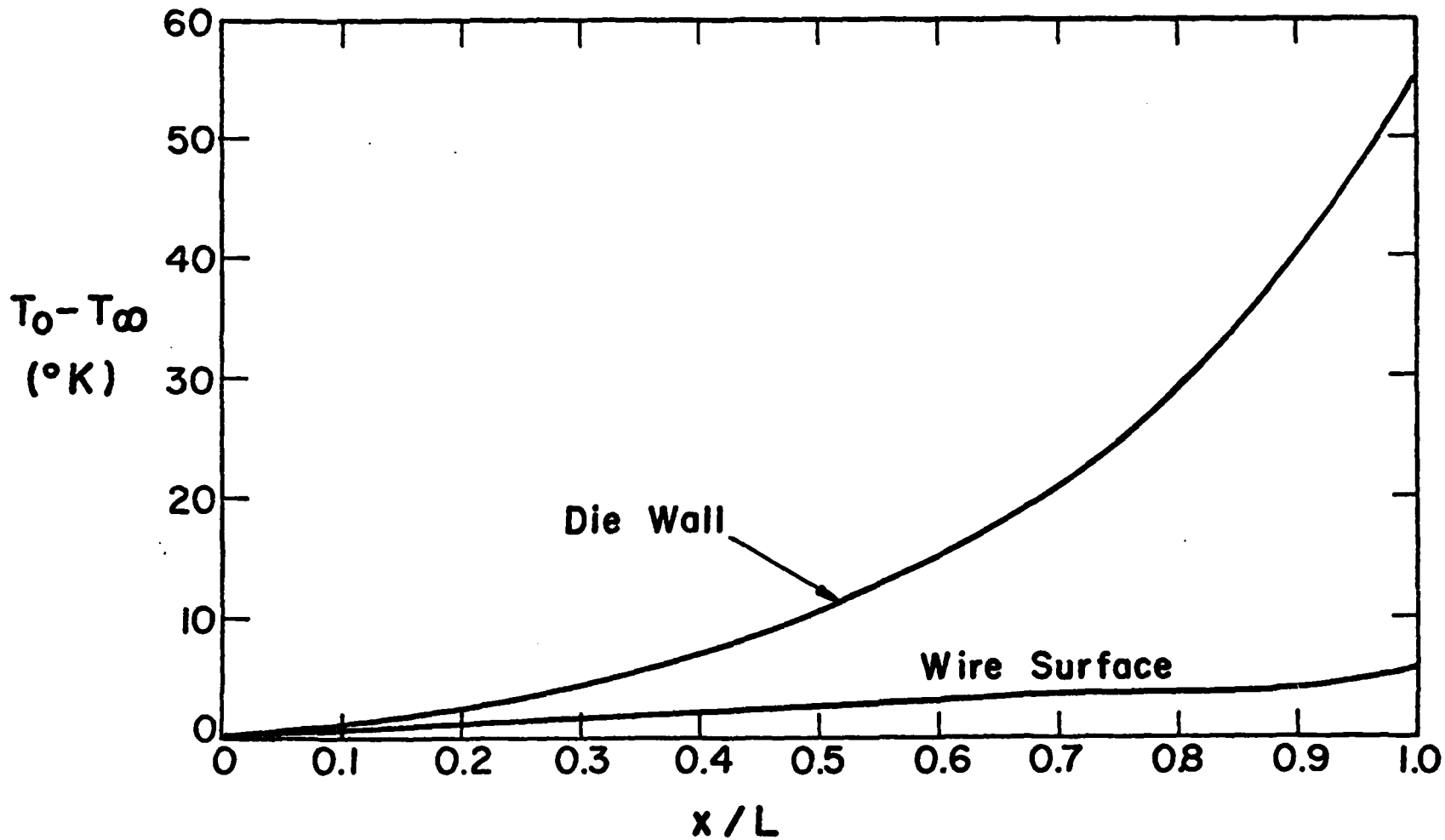

Figure 9. Surface temperature rises for an adiabatic wire-coating operation.

The boundary layer thickness associated with each increment of τ_0/h_z along the die wall is obtainable from Equations (32) and (86):

$$\delta(x,\xi) = \frac{1}{\sqrt{a\beta_d}} \left\{ 9\alpha \int_{x_1=\xi}^{x} \sqrt{a\beta_d}\, a\, dx_1 \right\}^{\frac{1}{3}} \tag{92}$$

Figure (10) shows the growth of five representative boundary layers emanating from equally spaced points along the die wall. Each of these layers grows rapidly at first, but then gets thinner as the flow converges and accelerates. The final thickness of the layer associated with the initial jump in τ_0 is 0.0011 inches (0.0028 cm) or 11% of the final coating thickness. Thus, the small-diffusivity assumption of the analysis is accurate here.

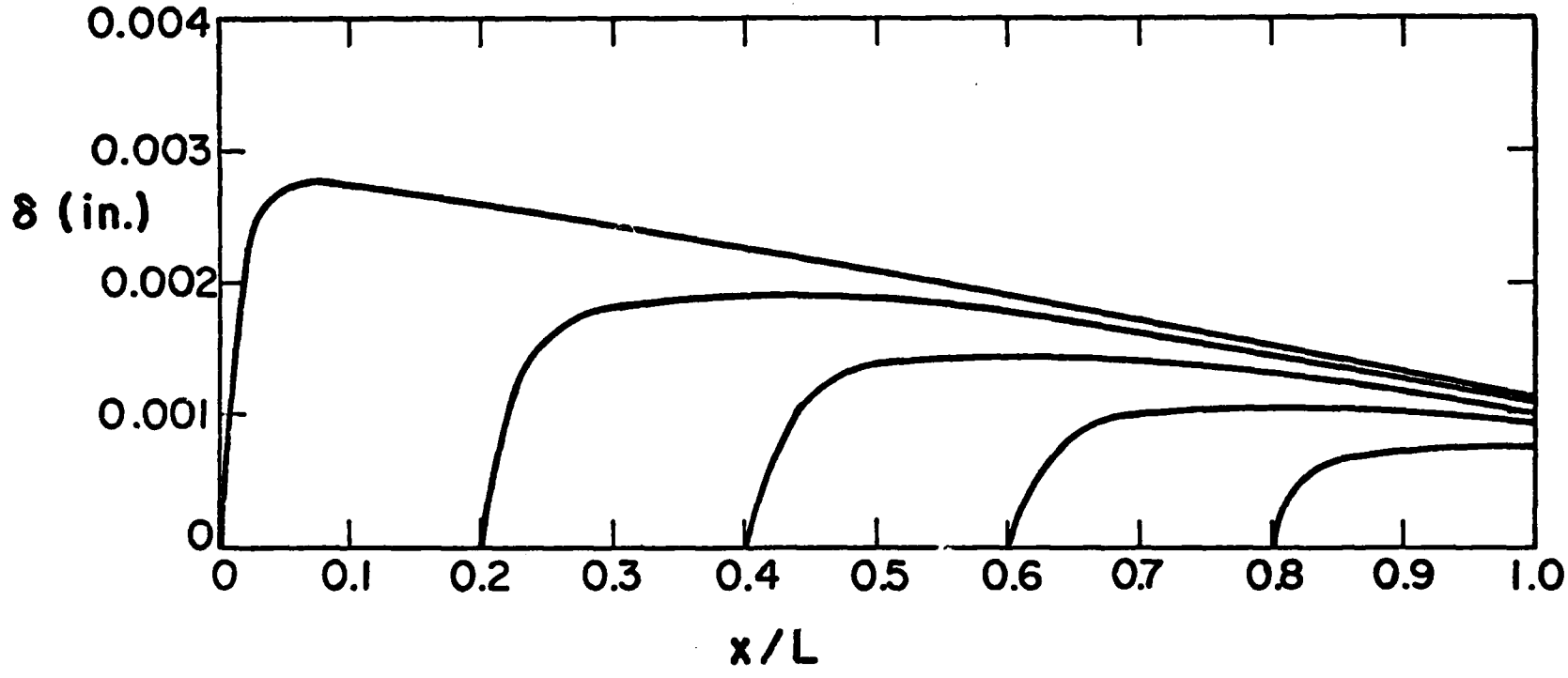

Figure 10. Thermal boundary layer development in a wire-coating system.

NOTATION

a = length of side of equilateral triangle; radius ratio in Eqs. (77)-(78).

$B(m,n)$ = $\Gamma(m)\Gamma(n)/\Gamma(m+n)$

$\hat{C}_p$ = heat capacity at constant pressure $(EM^{-1}T^{-1})$

$\frac{D}{Dt}$ = $\frac{\partial}{\partial t})_r + (V \cdot \nabla)$, substantial derivative

F = dimensionless function defined in Equation (66)

f = friction factor, see Equation (71)

f = function defined in Equation (23) (T)

$f''(0,m)$ = dimensionless shear stress at wedge surface, see Equation (56)

f_0, f_1, f_2 = dimensionless functions defined in Equation (79)

G = dimensionless function defined in Equation (67)

q = dimensionless temperature function defined in Equation (23)

h_x, h_y, h_z = scale factors defined in Equation (3)

k = thermal conductivity $(Et^{-1}L^{-1}T^{-1})$

L = length of channel

ℓ = arc length along a streamline

m = dimensionless parameter defined in Equation (58)

m_T = parameter in power law model, see Equation (88)

$O(y^n)$ = terms of order n or greater in y

P = $p + \rho\Phi$ $(ML^{-1}t^{-2})$

$P_0 - P_L$ = decrease of P along duct length L

Pr = Prandtl number

p = pressure $(M\ L^{-1}t^{-2})$

q_0 = conductive heat flux into the stream at $y = 0$ $(E\ L^{-2}t^{-1})$

R = gas constant ($E\ mole^{-1}T^{-1}$)

R = radius of sphere or cylinder

Re = Reynolds number

R_1 = wire radius

$R_2(x)$ = local radius of wire-coating die

$\underset{\sim}{r}$ = position vector

r = radial coordinate

r = dimensionless ratio C_1/C_0 , see Equation (34)

T = absolute temperature

U = local free stream velocity for wedge flow (Lt^{-1})

$\langle V \rangle$ = mean velocity through cross-section of pipe (Lt^{-1})

$\underset{\sim}{v}$ = velocity vector relative to non-deforming coordinates (Lt^{-1})

V = magnitude of velocity vector (Lt^{-1})

V_w = velocity of wire or moving wall (Lt^{-1})

V_x, V_y, V_z = components of velocity vector (Lt^{-1})

V_r, V_θ = velocity components in cylindrical or spherical coordinates (Lt^{-1})

V_t = tangential component of velocity vector (Lt^{-1})

V_∞ = magnitude of free stream velocity (Lt^{-1})

X_1, X_2, X_3 = material coordinates

x = surface coordinate directed along surface streamlines; see Equations (3)-(6) (Lh_x^{-1})

Y = half-width of slit (L)

y = normal distance from interface (L)

Z = cylindrical axial coordinate (L)

z = surface coordinate normal to the local x-direction; see Equations (3)-(6) (Lh_z^{-1})

Greek Symbols

α = $k/\rho\hat{C}_p$, thermal diffusivity (L^2t^{-1})

β = $(\partial v_t/\partial y)|_{y=0}$, function introduced in Equation (4) (t^{-1})

$\Gamma(x)$ = $\int_0^\infty e^{-z} z^{x-1} dz$

γ = Euler's constant, 0.57721...

δ = boundary layer thickness for viscous heating or heat transfer (L)

$\underset{\sim}{\delta}_x, \underset{\sim}{\delta}_y, \underset{\sim}{\delta}_z$ = unit vectors

ε = special dissipation function for fundamental solution, see Equations (19) and (43)

η = dimensionless coordinate defined in Equation (24)

θ = angle in cylindrical or spherical coordinates

θ = wedge angle (radians)

κ = ratio of inner cylinder radius to outer

μ = viscosity $(ML^{-1}t^{-1})$

ν = μ/ρ kinematic viscosity (L^2t^{-1})

ξ = value of x at the jump in ε and $T^{*(i)}$

Π = dimensionless temperature function in Equation (48)

ρ = density (ML^{-3})

σ = $(x/R)(R\langle V\rangle/\nu)^{-1}$, dimensionless downstream coordinate in tube

$\underset{\sim}{\tau}$ = stress tensor $(ML^{-1}t^{-2})$

τ_0 = magnitude of tangential stress at interface $(ML^{-1}t^{-2})$

$\hat{\Phi}$ = gravitational potential energy (L^2t^{-2})

ϕ = angle in spherical coordinates

ω = angular velocity of rotating disk (radians sec^{-1})

ψ_1, ψ_2 = stream functions, see Equation (7)

Superscripts

(i)	inner solution
(o)	outer solution
*	solution with special dissipation function $\varepsilon(x,\xi,z)$.

Subscripts

A	dissipative solution for adiabatic boundary
d	at die wall
w	at wire surface
0	in or into the fluid at $y = 0$
∞	upstream or initial state
1	dummy variable

LITERATURE CITED

Bird, R. B., W. E. Stewart, and E. N. Lightfoot, Transport Phenomena, Wiley, New York, (1960).

Bird, R. B., R. C. Armstrong, and O. Hassager, Dynamics of Polymeric Liquids: Vol I Fluid mechanics, Wiley, New York (1977).

Carley, J. F., T. Endo, and W. B. Krantz, "Realistic Analysis of Flow in Wire-Coating Dies", Society of Plastic Engineers, 36, 453 (1978).

Cochran, W. G., "The Flow Due to a Rotating Disc", Proc. Cambr. Phil. Soc., 30, 365 (1934).

Haas, K. U., and F. H. Skewis, "The Wire-Coating Process; Die Design and Polymer Flow Characteristics", Society of Plastic Engineers, 32, 8 (1974).

Hartree, D. R., "On an Equation Occurring in Falkner and Skan's Approximate Treatment of the Equations of the Boundary Layer," Proc. Camb. Phil. Soc., 33 , 223 (1937).

Hornbeck, R. W., "Laminar Flow in the Entrance Region of a Pipe', Applied Scientific Research, 13, 224 (1964).

Landau, L., and E. M. Lifshitz, Fluid Mechanics, Addison-Wesley, Reading, Massachusetts (1960).

Lighthill, M. J., Proc. Roy. Soc., A202, 359 (1950).

Meksyn, D., "Plate Thermometer", ZAMP , 11, 63 (1960).

Pohlhausen, E., "Der Wärmeaustauch zwischen festen Körpern und Flüssigkeiten mit kleiner Reibung and kleiner Wärmeleitung", ZAMM 1, 115 (1921).

Rosenhead, L., Laminar Boundary Layers, Oxford University Press, Oxford (1963).

Schlichting, H., Boundary Layer Theory, 4 ed., McGraw-Hill, New York (1960).

Stewart, W. E., "Forced Convection in Three-Dimensional Flows: I. Asymptotic Solutions for Fixed Interfaces", AIChE J., 9, 528 (1963).

Stewart, W. E., J. B. Angelo, and E. N. Lightfoot, "Forced Convection in Three-Dimensional Flows: II. Asymptotic Solutions for Mobile Interfaces", AIChE J., 16, 771 (1970).

MAM/WES/db

SECURITY CLASSIFICATION OF THIS PAGE (When Data Entered)

REPORT DOCUMENTATION PAGE		READ INSTRUCTIONS BEFORE COMPLETING FORM
1. REPORT NUMBER 2295	2. GOVT ACCESSION NO. AD-A110	3. RECIPIENT'S CATALOG NUMBER 45
4. TITLE (and Subtitle) FORCED CONVECTION IN THREE-DIMENSIONAL FLOWS: III. ASYMPTOTIC SOLUTIONS WITH VISCOUS HEATING		5. TYPE OF REPORT & PERIOD COVERED Summary Report - no specific reporting period 6. PERFORMING ORG. REPORT NUMBER
7. AUTHOR(s) Matthew A. McClelland and Warren E. Stewart		8. CONTRACT OR GRANT NUMBER(s) DAAG29-80-C-0041
9. PERFORMING ORGANIZATION NAME AND ADDRESS Mathematics Research Center, University of Wisconsin 610 Walnut Street Madison, Wisconsin 53706		10. PROGRAM ELEMENT, PROJECT, TASK AREA & WORK UNIT NUMBERS 2- Physical Mathematics
11. CONTROLLING OFFICE NAME AND ADDRESS U. S. Army Research Office P.O. Box 12211 Research Triangle Park, North Carolina 27709		12. REPORT DATE November 1981 13. NUMBER OF PAGES 40
14. MONITORING AGENCY NAME & ADDRESS(if different from Controlling Office)		15. SECURITY CLASS. (of this report) UNCLASSIFIED 15a. DECLASSIFICATION/DOWNGRADING SCHEDULE

16. DISTRIBUTION STATEMENT (of this Report)

Approved for public release; distribution unlimited.

17. DISTRIBUTION STATEMENT (of the abstract entered in Block 20, if different from Report)

18. SUPPLEMENTARY NOTES

19. KEY WORDS (Continue on reverse side if necessary and identify by block number)

Matched asymptotic solutions, Boundary layers, Viscous dissipation, Heat transfer

20. ABSTRACT (Continue on reverse side if necessary and identify by block number)

Asymptotic solutions are given for temperature profiles in laminar three-dimensional flows with viscous dissipation. The results are asymptotically valid for small thermal diffusivity α; they hold for Newtonian or non-Newtonian fluids. The fluid properties are evaluated at an average temperature for the system; this is satisfactory for moderate temperature differences. Heat transfer formulas for various thermal boundary conditions are included. The general formulas are applied to several geometries; numerical results are obtained for a wire-coating operation.

DD FORM 1 JAN 73 1473 EDITION OF 1 NOV 65 IS OBSOLETE

UNCLASSIFIED 22 12 00

SECURITY CLASSIFICATION OF THIS PAGE (When Data Entered)


DAT
FILM